

Hybrid Cavity for J-PARC Rapid Cycling Synchrotron

Alexander Schnase¹, Masahiro Nomura, Fumihiko Tamura, Masanobu Yamamoto

Center for Proton Accelerator Facility, JAERI, 2-4 Shirakata-Shirane, Tokai, Ibaraki, 319-1195, Japan
Shozo Anami, Eizi Ezura, Keigo Hara, Yoshinori Hashimoto, Chihiro Ohmori, Akira Takagi, Makoto Toda,
Masahito Yoshii, High Energy Accelerator Research Organization, 1-1 Oho, Tsukuba, 305-0801, Japan

Abstract

The operating of the cavities for the RCS at J-PARC is optimized for a Q-value of $Q=2$. This Q-value is reached by using a cut-core configuration of the magnetic alloy the cavities are loaded with. However, there is a technology limit, because the required cut size between 2 parts of each core is in the order of 1mm, which is comparable to core distortions and tolerances. Therefore we present the idea to combine cavity tanks with uncut cores ($Q=0.5\dots0.6$) in combination with cavity tanks with cut cores with a bigger gap and a Q-value of 4...5 to reach $Q=2$.

INTRODUCTION

The J-PARC complex [1], [2] will deliver high intensity protons at 3GeV to a neutron target and at 50 GeV to a target for neutrino studies. The 3GeV RCS (Rapid Cycling Synchrotron) [3] will accelerate protons from 181MeV to 3GeV in 20ms. The acceleration cavities, based on Magnetic Alloy (MA) require no tuning as compared to standard ferrite cavities [4], [5], [6].

Table 1: Main RF-Parameters of RCS and MR

	RCS	MR
Acceleration voltage	450 kV	280 kV
Acceleration frequency	0.94-1.67 MHz	1.67-1.72 MHz
Harmonic number	$h=2$	$h=9$ ($h=18$)
Energy	181-3000MeV	3-50GeV
Intensity	5×10^{13} ppp	3.3×10^{14} ppp
Average beam current	4~7A	11A
Number of cavities	11+1	6+1
Gaps per cavity	3	3
Voltage per gap	13.6kV	15.5kV
Q-value	~ 2	10~20

The RF-parameters for RCS and MR (50GeV Main-Ring) are comparable, as shown in table 1, [7]. The cavity structure is shown in figure 1. However, the bandwidth requirement, and therefore the Q-value is quite different. For MR operation, the Q-value of 10~20 requires a gap between both halves of the cut core in the order of 1cm, like in figure 2. For RCS operation and a Q-value 2, the distance between cut cores is approximately 1mm.

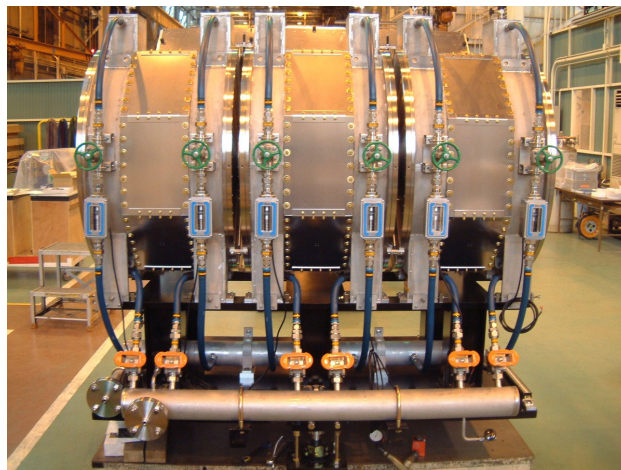


Fig. 1: The 3gap, 6tank, direct cooled cavity structure

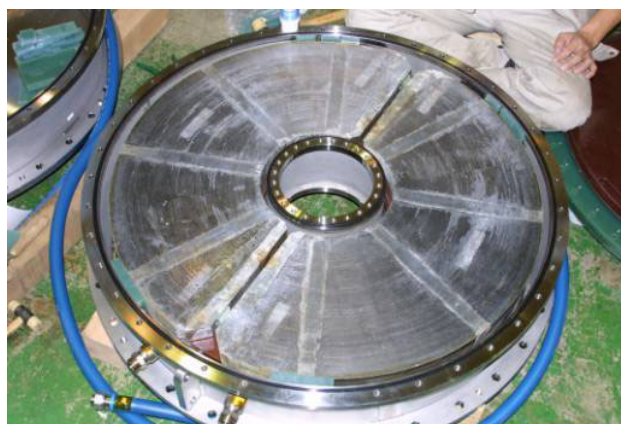


Fig. 2: One MR cavity tank with cut cores

If the Q value is higher than 2, it is difficult to cover ($h=2$) for acceleration and ($h=4$) for beam shaping within one cavity. If the Q value is too small, the cavity is too broadband and it is more difficult to compensate the beam loading at higher harmonics [5].

For $Q=2$, the distance between the 2 parts of each cut-core becomes less than 1mm. Under this condition, the roughness of the cutting surface influences the local heat distribution [8]. With water-jet cutting, the surface roughness combined with tolerances and the thickness of the coating against corrosion, allows us to reach a Q-value of 3...4, but not 2. Preventing excessive heat on the cut surface is important, because the cooling water cannot easily find a way to go through such a narrow gap.

¹ E-mail: a.schnase@fz-juelich.de

Grindstone cutting reduces local heating, because the cut surface is much smoother [8]. Still, we have mechanical tolerances; so we developed the idea of a Hybrid cavity.

2 HYBRID CAVITY

We present a model method that explains how to combine uncut cores with Q-value of 0.6 with cut-cores with Q-value of 4 to obtain an average Q-value of 2. We combine 6 cut-cores with a gap set for a Q-value around 4 in the 2 center tanks with 12 un-cut cores for the 4 outer tanks with a Q-value of 0.6. We can set enough gap space for the cut cores in this scheme.

2.1 Modelling the MA cores

The cores are made using a thin MA tape, wound up like a spiral. There is a silica isolation on one side of the tape to reduce effect of eddy currents. Measuring of the production cores is with an impedance meter and a one-turn loop. The loop is made of a thin and wide isolated copper foil to reduce the effect of the loop self-inductance. The impedance meter will give unreliable results in case of a resonance; therefore once the cores are assembled into a tank we use a network analyzer.

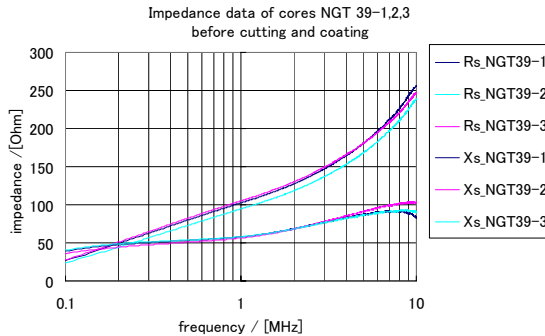


Fig. 3: Impedance data of MA-cores NGT 39-1, 2, 3 before cutting and coating

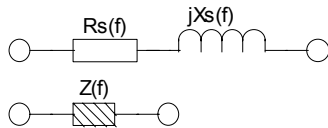


Fig. 4: Series impedance model of a core

The impedance data $Z = R_s + jX_s$ from 3 test cores NGT039-1, 2, 3 are plotted in fig. 3. The cores will be stacked; therefore a serial impedance model shown in fig. 4, for each core is preferred. The data in fig. 3 indicates, that R_s and X_s depend on frequency:

$$Z(f) = R_s(f) + j X_s(f). \quad (1)$$

The frequency dependence can be approximated by

$$R_s(f) = R_{s0} (f/f_0)^{b_R} \quad (2)$$

$$X_s(f) = X_{s0} (f/f_0)^{b_X}, \quad (3)$$

where $f_0=1$ MHz is chosen for convenience.

The raw data taken by network analyzer is corrected for the influence of the measurement set-up. There is a stray capacitance C_{par} between the measurement loop and

the core and an inductance L_{ser} , due to the connection of the measurement loop to the network analyzer.

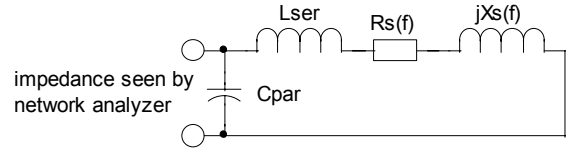


Fig. 5: Effects of the measurement set-up: L_{ser} and C_{par}

With the correction shown in fig. 5, $L_{ser}=0.65\mu\text{H}$ and $C_{par}=16\text{pF}$, we find the coefficients R_{s0} , X_{s0} , and the exponents b_R , and b_X for the approximations (2), (3). For the RMS error, we define:

$$RMS_{err} = \sqrt{\frac{1}{n} \sum_{i=1}^n (R_{s_meas_i} - R_s(f_i))^2 + (X_{s_meas_i} - X_s(f_i))^2} \quad (4)$$

The error of the approximation is $3\sim 4\Omega$ for frequencies below 400 kHz. For RCS operation the frequency range of the acceleration harmonic ($h=2$) is 0.94~1.67 MHz. Harmonic ($h=4$) is used for beam shaping, and the harmonics 1,3,5, and 6 are used for beam-loading compensation. Therefore, the approximation has to cover 0.47~5.01MHz. Headroom for higher frequencies is an advantage, because we have to consider the impedance of higher harmonics ($h>6$) for beam-loading effects. The RMS error in 0.47~10 MHz is less than 2Ω , which is acceptable for our purpose.

Table 2: Exponential approximation

Core NGT	R_{s0} [Ω]	X_{s0} [Ω]	b_R	b_X	RMS _{err} 0.1~10 MHz [Ω]	RMS _{err} 0.47~10 MHz [Ω]
39-1	98.09	56.21	0.3226	0.1947	3.19	1.57
39-2	91.43	54.07	0.3165	0.2362	3.25	1.45
39-3	101.9	56.24	0.2934	0.1905	3.84	1.78

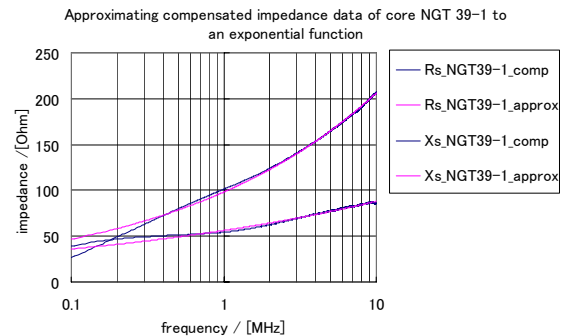


Fig. 4: Exponential approximation to NGT 39-1 data

The formulae (2), (3) are helpful for numerical calculation. Another way to represent the cores is with lumped frequency independent elements R, L, and C. This allows electric circuit simulator simulations. The data in fig. 3 shows that more than one frequency independent R-L lumped element is necessary for good approximation. Empirically, a circuit with 3 resistors and

3 inductors is a compromise between complexity and $RMS_{err}=2\Omega$. Fig. 5 shows the 2 dual choices of a model of one core.

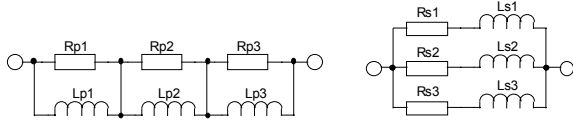


Fig. 5: 3 Series cells ($R_p||L_p$); 3 parallel cells ($R_s+j\omega L_s$)

For core NGT-39-1, the values are: $R_{p1}=81.4\Omega$, $R_{p2}=63.3\Omega$, $R_{p3}=153.6\Omega$, $L_{p1}=77.5\mu H$, $L_{p2}=6.62\mu H$, and $L_{p3}=2.11\mu H$ with $RMS_{err}=1.83\Omega$.

2.2 Applying the core model to the hybrid cavity

We combine the models of 3 cores for the 4 outer cells of the cavity (core1 to core 12) with a ($Q=4$) resonator model for the 2 center cells, as shown in fig. 6. The tanks are connected with bus bars. The impedance of the bus bars is small compared to the cavity impedances, therefore the tanks 1, 3, 5 and 2, 4, 6 look like connected in parallel. For push-pull operation, the simplified circuit structure with relocated gap capacitors is shown in fig. 7.

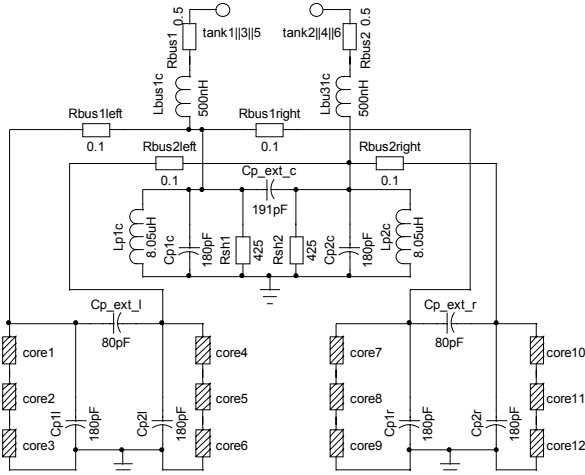


Fig. 6: The model for the combined tanks

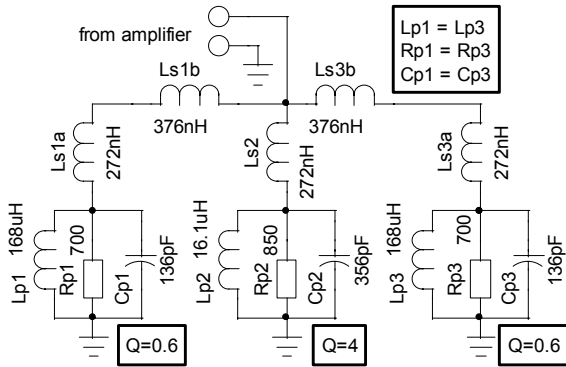


Fig. 7: The hybrid cavity structure

The push-pull impedance of the model in fig. 6 is compared in figure 8 to a simple resonator with $f_0=1.7$ MHz, $Q=2$ and shunt resistance of 275Ω .

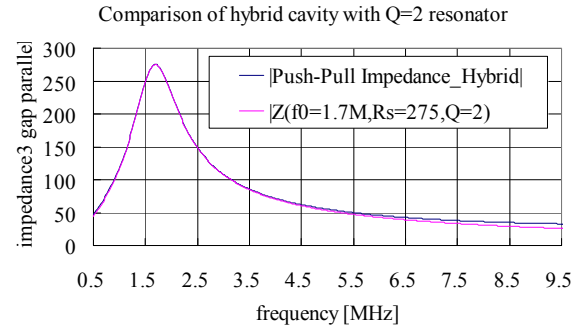


Figure 8: The impedance of the hybrid cavity structure

We notice, the similar behaviour of the hybrid cavity like a homogenous cavity with $Q=2$. The gap capacitors are not associated with the place they are installed. The power distribution between the tanks is a function of shunt resistance. As long as the shunt resistance of the tanks with the uncut cores is not much different from the tanks with the cut-cores, we expect a good power balance. In case of the un-cut cores we have to be aware of the radial heat distribution of the individual core, which has a maximum near the inner radius.

3 OUTLOOK

Currently, we are testing a scheme where all 6 tanks are filled with un-cut cores. We have reached $30kV_{pp}$ per gap, with an impedance of around 210Ω with 3 gaps in parallel. When the grindstone cutting of the large cores has reached production status, we can test the hybrid cavity configuration under realistic RCS operating conditions. Then we prepare the hybrid cavities for installation into RCS.

REFERENCES

- [1] <http://jkj.tokai.jaeri.go.jp/>
- [2] "Accelerator Technical design Report For High-Intensity Proton accelerator Facility Project, J-PARC", JAERI-Tech 2003-044
- [3] Y. Irie, "Challenges facing the Generation of MW Proton Beams using Rapid Cycling Synchrotrons", EPAC 2004, Lucerne, Switzerland
- [4] C. Ohmori et al., "High Field Gradient Cavity for J-PARC 3 GeV RCS", EPAC 2004
- [5] M. Yamamoto et al., "Dual Harmonic Acceleration with Broadband MA Cavities in J-PARC RCS", EPAC 2004
- [6] T. Uesugi et al., "Direct-Cooling MA Cavity for J-PARC Synchrotrons", PAC 2003
- [7] M. Yoshii, "Present status of J-PARC Ring RF Systems", PAC2005, Knoxville
- [8] M. Nomura et al., "Development of cutting technique of Magnetic alloys core", Proceedings of the 30th Linear Accelerator Meeting in Japan, Tosu, July 20-22, 2005